

Electronic Supplementary Information

Experimental Section

Fabrication of NiCu-LDH: The carbon cloth (CC) was treated with concentrated HNO_3 at $100\text{ }^\circ\text{C}$ for 3 h, then washed with ethanol and deionized water several times. Firstly, 2.5 mmol $\text{Ni}(\text{NO}_3)_2 \cdot 6\text{H}_2\text{O}$, 1.5 mmol $\text{Cu}(\text{NO}_3)_2 \cdot 3\text{H}_2\text{O}$, 8 mmol NH_4F and 20 mmol urea were dissolved in 80 mL deionized water to form a mixed solution. After being stirred evenly, the mixture with a piece of carbon cloth ($2 \times 2\text{ cm}^2$) was transferred to a 100 mL Teflon-lined stainless steel autoclave and heated to $120\text{ }^\circ\text{C}$ for 6 h. The obtained green samples were cleaned with deionized water and ethanol for several times.

Fabrication of Cu-doped NiFe-LDH: 3 mmol $\text{FeCl}_3 \cdot 6\text{H}_2\text{O}$ was dissolved in 50 mL deionized water to prepare iron chloride solution. The obtained NiCu-LDH was immersed in FeCl_3 solution. After that, the yellow product washed with ethanol and deionized water several times, and dried at $60\text{ }^\circ\text{C}$ overnight. The chemical bath time was set at 4, 6, 8, 10 hours.

Fabrication of C-NiFe-LDH, H-NiFe-LDH: For comparison, we treated $\text{Ni}(\text{OH})_2$ with the same chemical bath method, and the products were named as C-NiFe-LDH. The preparation of $\text{Ni}(\text{OH})_2$ was followed by the same way above except that we only add $\text{Ni}(\text{NO}_3)_2 \cdot 6\text{H}_2\text{O}$. Also, H-NiFe-LDH was synthesized by a simple one-step hydrothermal technique. The synthesis procedure of NiFe-LDH was similar to that for the NiCu-LDH, while the raw material is $\text{FeCl}_3 \cdot 6\text{H}_2\text{O}$ rather than $\text{Cu}(\text{NO}_3)_2 \cdot 3\text{H}_2\text{O}$.

Characterizations

XRD analysis with $\text{Cu K}\alpha$ radiation was done on X'PERT (Panalytical). The nanostructure, morphology was observed using SEM (Merlin Compact) and TEM (Tecnai G2 F30). The chemical composition of the sample was examined by XPS (Thermo Fisher Scientific ESCALAB 250 Xi, $\text{Al K}\alpha$ radiation).

Electrochemical measurements

All electrochemical performances were measured in the electrochemical workstation (CHI 760E). The OER properties were measured in a standard three-electrode system, using $1 \times 1\text{ cm}^2$ obtained samples, Hg/HgO and carbon rod as working electrode, reference electrode and counter electrode, respectively. All potentials applied were calibrated to a reversible hydrogen electrode (RHE) using the equation: $E_{\text{RHE}} = E_{\text{Hg/HgO}} + 0.059\text{ pH} + 0.098$. When the current density is j , the corresponding overpotential (η) of OER is followed by the equation: $\eta_j = E_j(\text{RHE}) - 1.23\text{ V}$. The polarization curves were measured at 2 mV s^{-1} , and were compensated with iR -correction. Before OER tests, all samples were cycled at 10 mV s^{-1} until the stability of cyclic voltammetry (CV), then the data were collected. The electrochemically active surface areas (ECSAs) of the OER were derived by performing CV measurements in a potential window of 1.13-1.23 V vs. RHE at different scan rates of 10, 20, 30, 40, 50 and 60 mV s^{-1} . Electrochemical impedance spectroscopy (EIS) was performed at a frequency range of 10^5 Hz to 0.01 Hz . The stability test was performed using the multistep method.

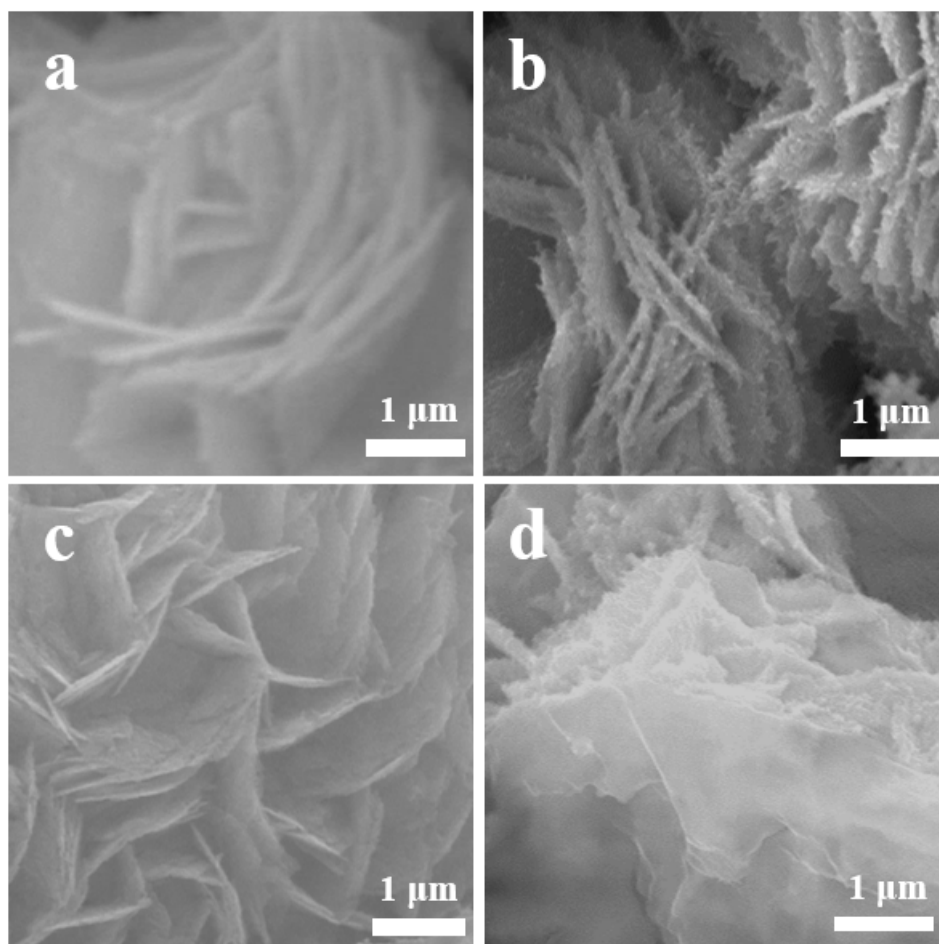


Fig. S1. SEM images of (a) NiFe-LDH|Cu-4h, (b) NiFe-LDH|Cu-6h, (c) NiFe-LDH|Cu-8h, (d) NiFe-LDH|Cu-10h.

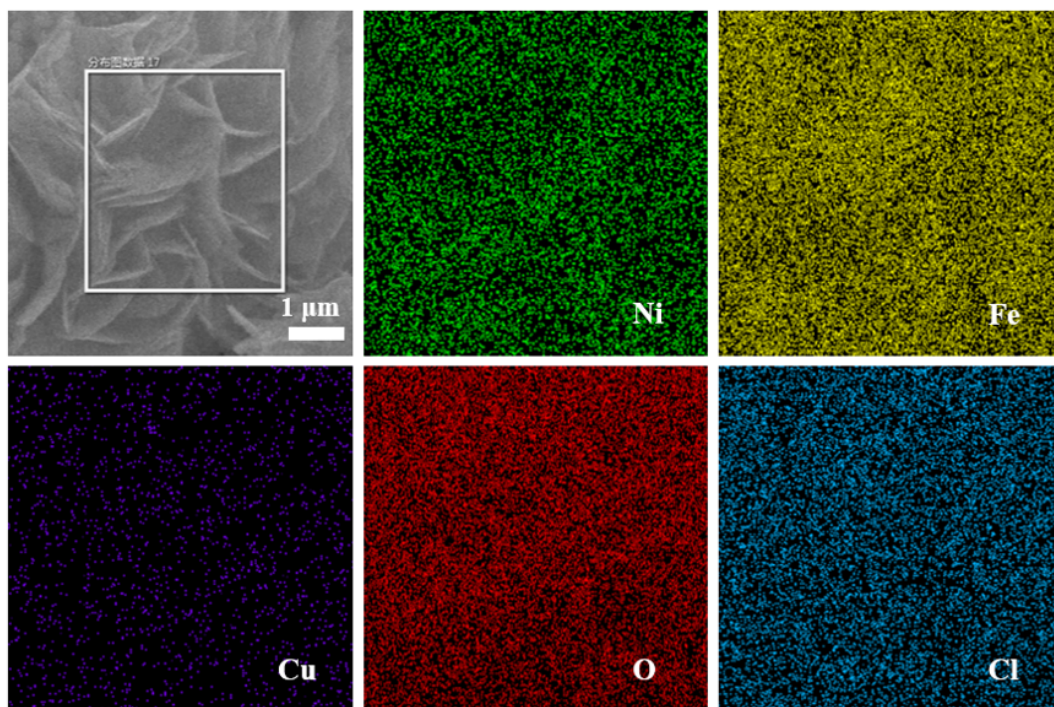


Fig. S2. Corresponding element mapping in NiFe-LDH|Cu.

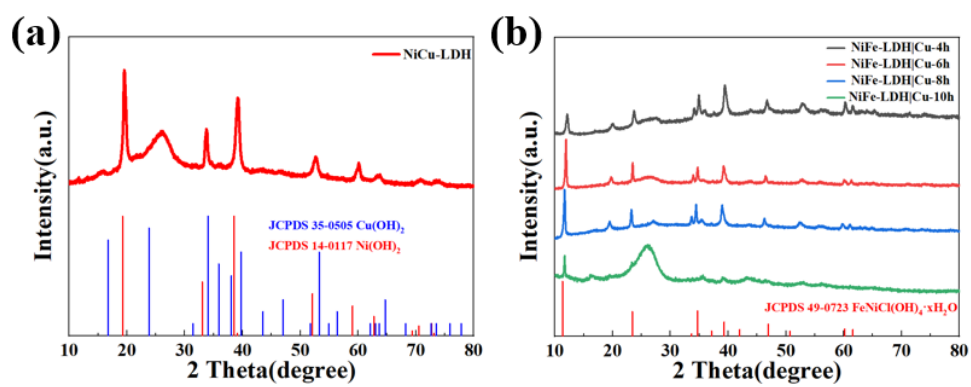


Fig. S3. XRD patterns of (a) NiCu-LDH, (b) NiFe-LDH|Cu samples under different reaction time.

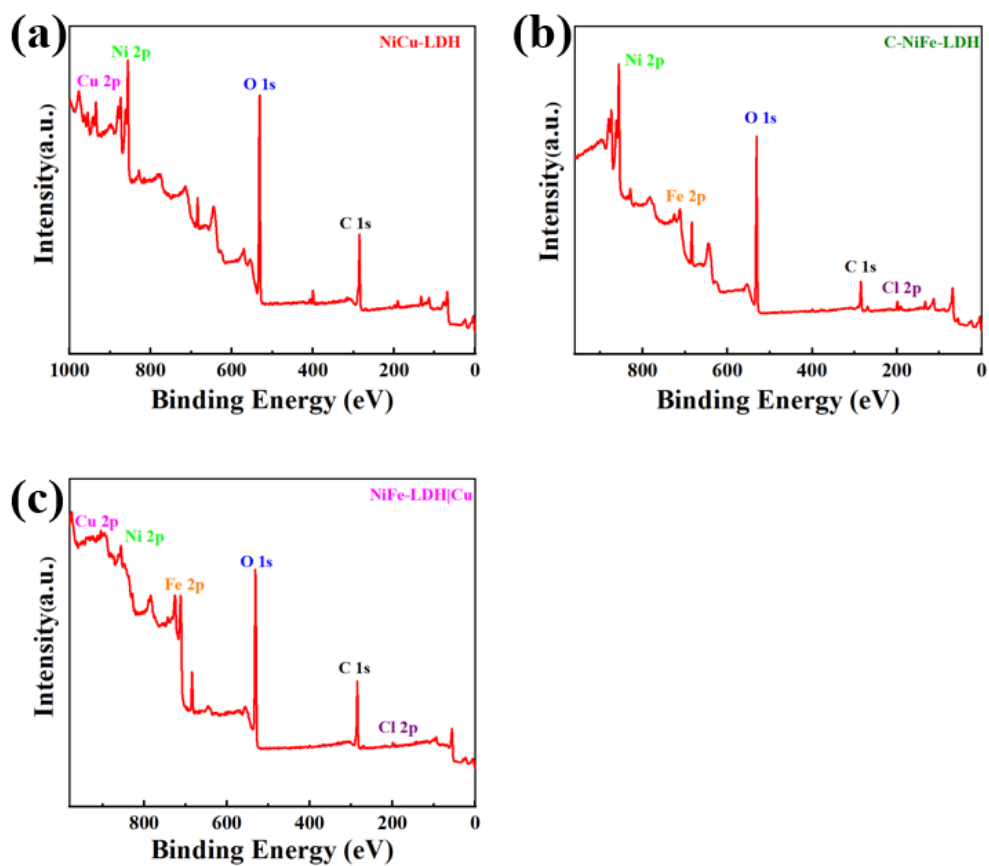


Fig. S4. XPS survey patterns of (a) NiCu-LDH, (b) C-NiFe-LDH, (c) NiFe-LDH|Cu.

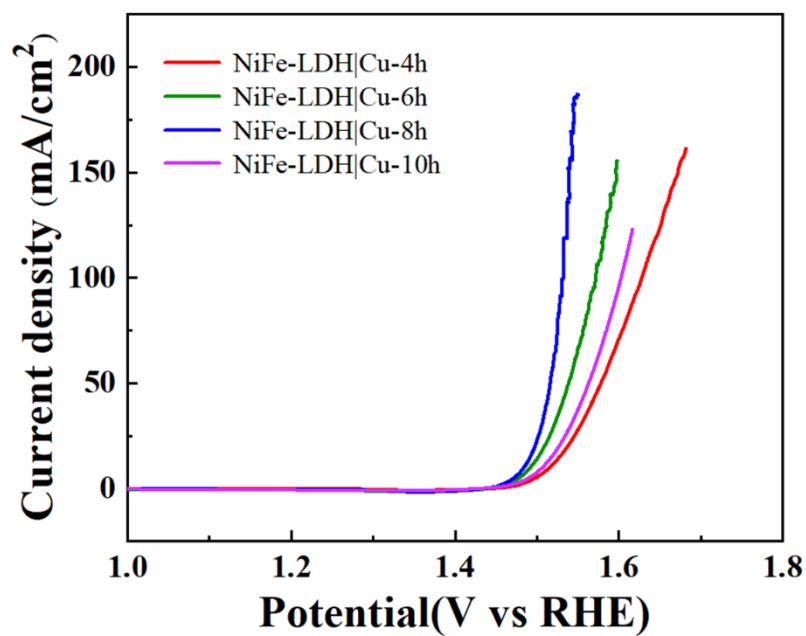


Fig. S5. LSV polarization curves of NiFe-LDH|Cu.

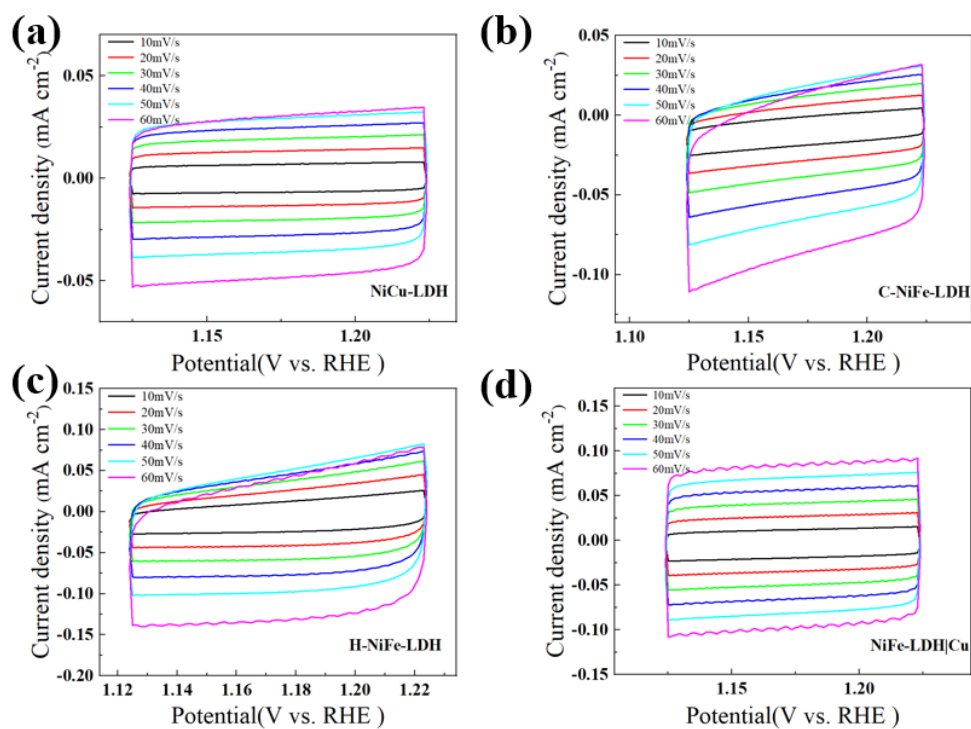


Fig. S6. CV curves of obtained samples for estimating the Cdl in OER tests.

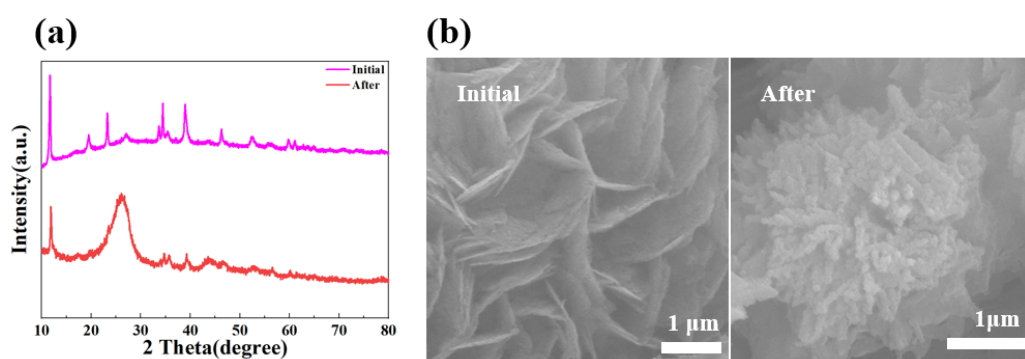


Fig. S7. (a) XRD patterns and (b) SEM images of NiFe-LDH|Cu after long cycling.

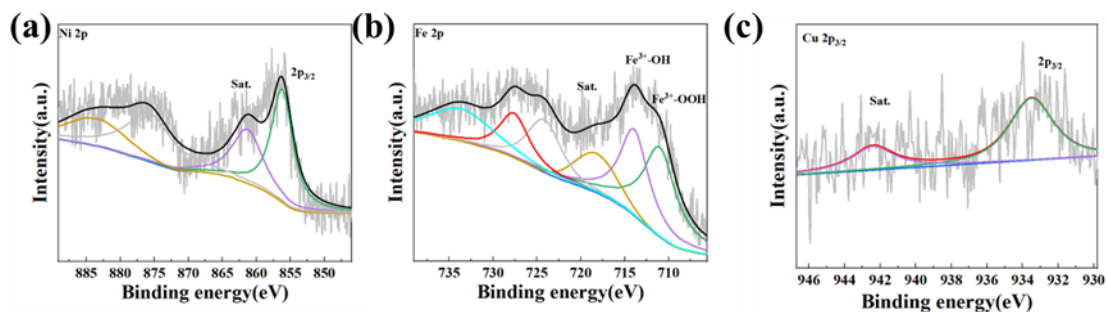


Fig. S8. XPS fine spectra of NiFe-LDH|Cu after long cycling (a) Ni 2p, (b) Fe 2p, (c) Cu 2p_{3/2}.

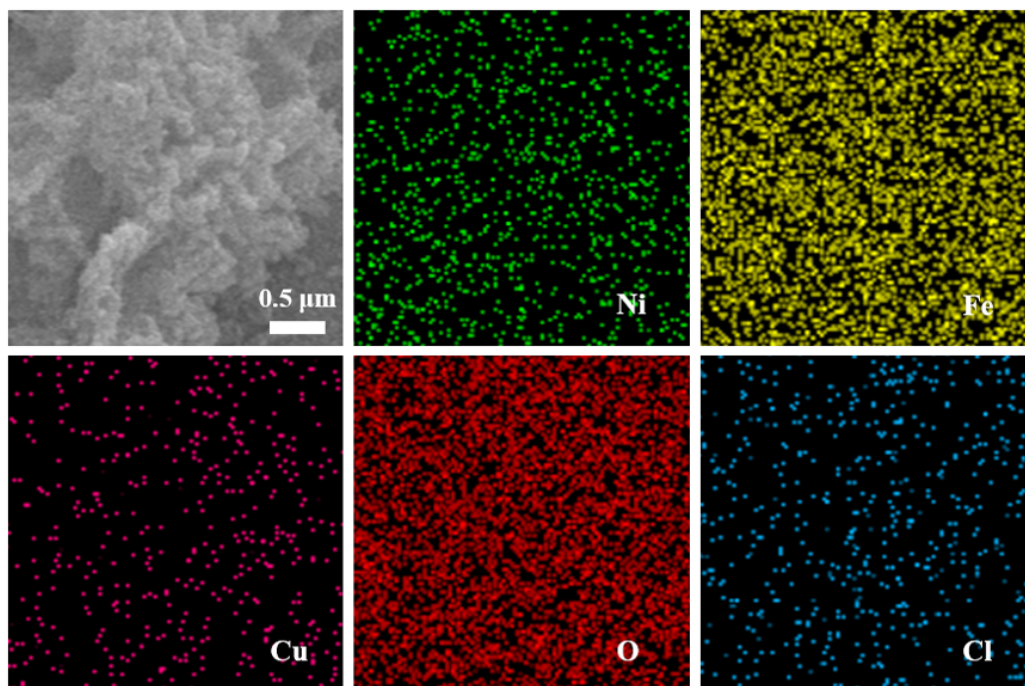


Fig. S9. Corresponding element mapping in NiFe-LDH|Cu after long cycling.

Table. S1 Comparison of OER performances for NiFe-LDH|Cu with previously reported electrocatalysts in the alkaline media.

Electrocatalyst	Electrolyte	Overpotential (mV)	Tafel slope (mV dec ⁻¹)	Ref
NiFe-LDH Cu	1.0 M KOH	253 at 10 mA cm ⁻²	42.9	This work
NiCo ₂ S ₄ @NiFe LDH	1.0 M KOH	287 at 10 mA cm ⁻²	46.5	[1]
Mo-NiFe-LDH	1.0 M KOH	317 at 20 mA cm ⁻²	44	[2]
NiFeV-LDH	1.0 M KOH	287 at 10 mA cm ⁻²	53.7	[3]
La-Cu(OH) ₂ -NiCo LDH	1.0 M KOH	254 at 10 mA cm ⁻²	148	[4]
Ru- NiFe-LDH	1.0 M KOH	246 at 10 mA cm ⁻²	67.2	[5]
CuO@NiCo LDH	1.0 M KOH	256 at 20 mA cm ⁻²	91	[6]

NiFe-LDH/NiCo ₂ O ₄	1.0 M KOH	363 at 50 mA cm ⁻²	53.0	[7]
Cu-CoFe-LDH	1.0 M KOH	253 at 10 mA cm ⁻²	63	[8]
FeCoNi-LDH	1.0 M KOH	299 at 10 mA cm ⁻²	53	[9]
NiCu-LDH	1.0 M KOH	290 at 10 mA cm ⁻²	42.5	[10]

If not mentioned specifically, all overpotentials were corrected with iR compensation.

Reference

- [1] Applied Catalysis B: Environmental 286 (2021) 119869.
[2] Materials Today Sustainability 17 (2022) 100101.
[3] Adv. Funct. Mater. 2021, 31, 2009743.
[4] International journal of hydrogen energy 47 (2022) 27996 e28006.
[5] Journal of The Electrochemical Society, 2022 169 024503.
[6] Inorg. Chem. Front., 2021, 8, 3049–3054.
[7] Journal of Physics and Chemistry of Solids 166 (2022) 110730.
[8] International journal of hydrogen energy 47 (2022) 9876 e9894.
[9] Energy Fuels 2020, 34, 11628–11636.
[10] Electrochimica Acta 282 (2018) 735-742.

Table. S2 The areal loading of NiCu-LDH, C-NiFe-LDH, H-NiFe-LDH and NiFe-LDH|Cu

Samples	The areal loading(mg cm ⁻²)
NiCu-LDH	1.9
C-NiFe-LDH	1.6
H-NiFe-LDH	2.2
NiFe-LDH Cu	1.2